Human Occlusion in Ultra-wideband Ranging: What Can the Radio Do for You?

Vu Anh Minh Le, Matteo Trobinger, Davide Vecchia, Gian Pietro Picco
University of Trento (Italy), {vuanhminh.le, matteo.trobinger, davide.vecchia, gianpietro.picco}@unitn.it

***Abstract*—Applications of ultra-wideband (UWB) for distance estimation (ranging) and localization often involve users wearing tags. Unfortunately, the human body causes significant signal attenuation, reducing ranging accuracy. This specific case of non-line-of-sight (NLOS) condition has received little attention in the literature. Further, state-of-the-art techniques tackling generic NLOS are often based on machine learning, limiting their exploitation on embedded devices. We pursue an alternative approach and show that the features offered by the UWB transceiver, largely neglected by the literature, can be *directly* exploited to reliably detect human occlusions and optimize ranging accordingly. We base our findings on an extensive experimental campaign exploring many radio, system, and deployment dimensions in two environments, resulting in practical guidelines immediately available to the designers of UWB-based systems.**

***Index Terms*—ultra-wideband, ranging, human occlusion**

I. Introduction

Recent years have seen a surge of interest for ultra-wideband (UWB) radios, ignited by the popular DW1000 by Decawave (now Qorvo). This is due to their ability to perform accurate, decimeter-level distance estimation (*ranging*), offering in a single transceiver two key elements—communication and localization—of several modern application scenarios.

Motivation. Many of these are human-centric, with the UWB device *worn* by a person, as in two staple examples from our group. Janus [1] detects proximity of the worn device to others on people or objects, enabling, e.g., hazard warnings in industrial contexts or social studies and contact tracing [2]. This requires estimating the *distance* between devices, commonly achieved via two-way ranging (TWR) [3]. Instead, the user *position* acquired by TALLA [4], our time-difference-of-arrival (TDoA) localization system, enables the extraction of stop-move patterns from museum visitor trajectories in [5].

In both cases, the user wears the device on the chest, attached to a lanyard; a simple, non-invasive solution [6]. Still, our in-field experiences show that *the presence of a human body on the UWB link induces a significant attenuation, decreasing the accuracy of ranging and localization* well below the decimeter-level typical of line-of-sight (LOS) conditions.

Dealing with NLOS in UWB is actively researched; yet, the state of the art (§II) evidences two problems. First, the focus is primarily on NLOS induced by the environment (e.g., walls or other obstacles); human occlusion received much less attention, despite its practical relevance. Second, techniques often rely on the channel impulse response (CIR) used by UWB radios for distance estimation, analyzed via machine learning; this induces tight computational (i.e., energy) constraints, limiting on-board exploitation on embedded devices.

Goal. This work tackles both problems above by *i)* focusing on the NLOS caused by human occlusion, HNLOS hereafter, and *ii)* exploiting only information directly available from the UWB radio without extra resource constraints.

Crucially, the popular DW1000 transceiver we exploit offers optimizations and indicators that, according to the manufacturer [7, 8], can be used to *mitigate* and *detect* NLOS conditions, respectively. However, again, these are largely ignored by the literature on UWB NLOS, leaving unclear to what extent they are effective, let apart in the case of HNLOS.

Experimental setup and methodology. We fill this gap with our study. We focus on ranging with TWR (§III), although the findings largely apply to TDoA, and consider four DW1000 optimizations (§IV): *i)* the default for LOS conditions *ii)* a variation with a longer 1024-symbol preamble, to improve signal reliability, and the ones recommended by the manufacturer for *iii)* mixed LOS-NLOS, and *iv)* NLOS conditions.

We assess their performance via experiments across several combinations of channels, distances, and device placement (§V). These are performed with one device occluded by the chest of the user (HNLOS) and, as a baseline, without it (LOS); we also consider the case with the human body behind the device, yielding LOS yet possibly affecting the signal (HLOS). Devices are either at same height, as when worn by People in proximity-based applications [1], or with non-occluded ones on the Ceiling, like localization anchors [5]. We also study HNLOS on the TWR initiator vs. the responder. To limit the effort to explore these many dimensions with good repeatability we focus on a single link. However, we analyze it in two real-world environments with different characteristics: a narrow Corridor and a large Hall at our university.

We ascertain the impact of the (many) combinations above on *i)* the reliability and accuracy of *ranging* (§VI), and *ii)* the ability of recommended radio indicators, i.e., power difference (PD) and confidence level (CL), to correctly *detect* line-of-sight conditions (§VII). To the best of our knowledge, we are the first to study how the features of UWB radios can be used directly to tackle HNLOS. Our salient findings (§VIII-A) can be immediately exploited in UWB-based systems, without the constraints of machine learning techniques, and inspire follow-up research, as outlined in our concluding remarks (§IX).

II. Related Work

Recent works tackle detection and mitigation of NLOS errors by analyzing the channel impulse response (CIR) available to the programmer in UWB chips. Two main approaches exist. The first one extracts key features from the CIR, e.g., energy levels in specific areas, mean excess delay and its spread in multipath components, or kurtosis. These are used directly to detect the link condition [9] or input into a machine learning module for detection and/or error mitigation, e.g., Support Vector Machines [10], Support Vector Regression (SVR) [11], or regression trees [12]. Instead, the second approach directly injects the full CIR into a convolutional network [13, 14] trained with CIR signals. Unfortunately, acquiring and processing the CIR signal is taxing in terms of latency and energy consumption. An alternative to using the CIR is to aggregate multiple ranging results, exploiting only their estimated distance and RX power level to classify link conditions via k-Nearest Neighbors (k-NN), Support Vector Machines (SVM), or Gaussian processes [15]. This simpler strategy avoids the CIR overhead but requires multiple ranging exchanges, still increasing latency and energy consumption.

Moreover, efforts in NLOS detection and mitigation focus on obstructions from walls or large objects, mostly neglecting HNLOS. Still, the human body is known to heavily affect UWB ranging accuracy, especially when the antenna is close to the body, as in wearable devices. Chest occlusion, our focus, causes large errors [1, 16] affecting applications using this common position for the user tag [1, 4, 6]. The few works studying human occlusion, e.g., [12], neither analyze the many radio aspects impacting performance nor propose solutions to mitigate them. The work in [17] proposes a method based on the power difference indicator, but does not evaluate the others available on the DW1000, i.e., the confidence level and its sub-components (§IV). Finally, the impact of different radio optimizations and frequency channels is still unexplored. To the best of our knowledge, we are the first to investigate extensively how all these radio characteristics can be exploited for ranging in the presence of human occlusions.

III. UWB Ranging in a Nutshell

Basics. We use DWM1001 modules by Decawave (now Qorvo), equipped with the popular DW1000 UWB radio. This chip exploits standard preamble symbols designed to have perfect periodic autocorrelation [18], enabling acquisition of the channel impulse response (CIR) upon packet reception (RX). The CIR is then processed on-chip via a proprietary leading edge detection (LDE) algorithm that locates the first path of the incoming signal and accurately determines its RX timestamp. During preamble RX the radio also estimates the carrier frequency offset (CFO), yielding the clock drift δ between receiver and transmitter. Finally, the radio can schedule transmissions (TX), computing the timestamp beforehand. Together, these properties enable accurate ranging.

Ranging. The signal time of flight τ, multiplied by the speed of light c, yields a distance estimate. We consider single-sided two-way ranging [3], the most common approach, involving two packets: a POLL sent by the initiator I and a RESPONSE sent back by the responder R. The estimation of τ relies on four timestamps (Figure 1). The responder schedules the

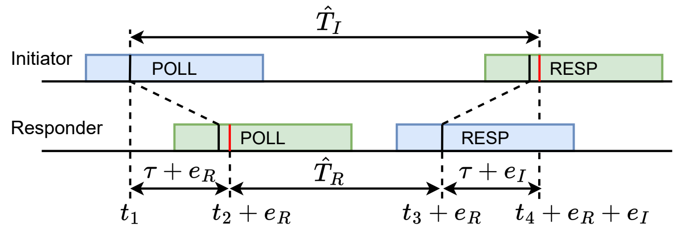

Fig. 1. Single-sided two-way ranging.

RESPONSE in advance, embedding the TX timestamp t_3 into the packet, based on which the initiator computes

$$\tau = \frac{1}{2}(T_I - T_R) = \frac{1}{2}((t_4 - t_1) - (t_3 - t_2)) \tag{1}$$

Accuracy is affected by the clock drift between I and R and RX timestamping errors. If clocks have an offset δ w.r.t. their nominal frequency and RX timestamps are subject to an error e, the actual time intervals in (1) are $\hat{T}_R = T_R(1 + \delta_R)$ and $\hat{T}_I = T_I(1 + \delta_I) + e_R + e_I$. The initiator can compensate the clock drift by a factor $\bar{\delta} \approx \delta_I - \delta_R$ by relying on CFO estimation [19]. Therefore, considering that $\tau \ll T_R$, yielding $T_R \approx T_I$, estimates are affected only by timestamping errors

$$\hat{\tau} = \frac{1}{2}(\hat{T}_I - \hat{T}_R) \approx \frac{1}{2}(T_I + e_R + e_I - (1 - \bar{\delta})T_R) \tag{2}$$

where e_I and e_R depend on *i)* the bias induced by distance and relative orientation of nodes, and *ii)* line-of-sight conditions. The former causes decimeter-level inaccuracies and is present regardless of the latter; its correction is outside the scope of this work. Instead, our focus is on the source of error in HNLOS conditions, yielding meter-level inaccuracies.

Similar considerations hold for other ranging or localization schemes. For example, HNLOS causes RX timestamp errors on links to TDoA anchors, akin to those in TWR; many of our findings (§VIII-A) are therefore directly applicable.

IV. Radio Features to Counter Human NLOS

Optimizations. The manufacturer guidelines to optimize the DW1000 for given line-of-sight conditions [20, 21] rely on two main parameters. The first one is the *noise multiplier* of the LDE algorithm. When executing the latter, the radio first finds the CIR region with the lowest noise, whose value then multiplied by a configurable factor yields the threshold used to detect the signal first path and its time of arrival. A high multiplier may cause the first path to be missed when the signal is attenuated, typical in NLOS (Figure 2); a low multiplier enables detection despite attenuation but yields more incorrect ranging estimates, as noise can be mistaken for the first path.

The second one is the number of symbol repetitions in the preamble sequence of a transmitted packet, or *preamble length*. A long preamble increases the reliability of the LDE outcome by allowing the receiver to accumulate many symbols in the CIR; these also provide more samples enabling better CFO estimates $\bar{\delta}$. However, these benefits come with an increase of ranging time and energy consumption.

Based on this, we consider four radio optimizations:

- cLOS uses the highest noise multiplier and a 128-symbol preamble. It is the default in the DW1000 device driver ([7], p. 175) and is meant for LOS conditions.
- cMIXED is similar to cLOS, but uses a lower noise multiplier; it is meant for mixed LOS/NLOS conditions.
- cNLOS uses the lowest noise multiplier and a 1024-symbol preamble. It improves ranging estimates in NLOS conditions but is prone to spurious ones [21].
- cLOS_{1024} is our variant of cLOS using a 1024-symbol preamble. We explore its potential to mitigate ranging errors as in cNLOS but without spurious estimates.

Link-level indicators. The DW1000 offers two indicators for detecting line-of-sight conditions. The *power difference (PD)* is computed from the CIR when receiving a preamble, as the difference $PD{=}RSS{-}FPPL$ between the total RX signal strength and the one of the first path peak. According to the manufacturer [7], the link is in LOS when $PD < 6$ dBm and NLOS when $PD > 10$ dBm; uncertain otherwise. Intuitively, a low PD indicates that most of the signal energy received remained in the first path, unaffected by noise or reflections.

The *confidence level (CL)* is more complex, and depends on three sub-components, evaluated in order. The likelihood of undetected early path ($LUEP$), is computed by analyzing few CIR samples before the first path. If $LUEP > 0$ the first path may have been missed by the LDE threshold, hinting at NLOS; CL is set to the minimum of 0. If $LUEP = 0$, the probability of NLOS ($PrNLOS$) is evaluated based on the time interval ΔT between the detected first path and the CIR peak with highest amplitude. A large ΔT indicates that the receiver is subject to strong and late reflections, usually observed in NLOS. If $PrNLOS = 0$, CL is set to the maximum of 1. Otherwise, another component (M_C) is considered, indicating whether the CIR accumulator has saturated. This typically happens in LOS but is unlikely to happen in NLOS, since the incoming signal is attenuated. If M_C indicates saturation, $CL = 1$, otherwise $CL = (1 - PrNLOS)$.

Finally, we define our own variant CL^* that disregards $LUEP$, as we observe (§VII) that when a low noise multiplier is used, $LUEP > 0$ is often caused by noise rather than NLOS.

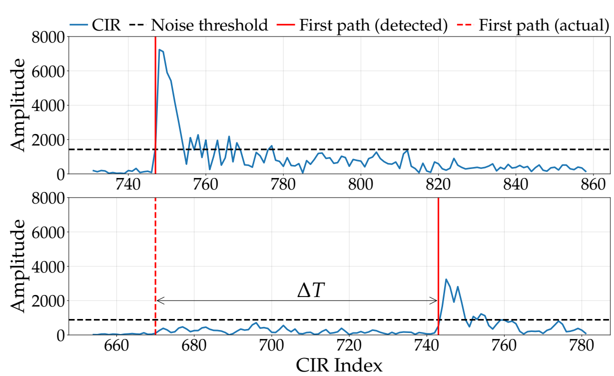

Fig. 2. In LOS (top), the first path is correctly detected from the CIR. In HNLOS (bottom), it is severely attenuated by body occlusion, causing a later reflection to be detected instead.

V. Experimental Settings

We explore the combined impact of several key deployment and system parameters (Table I), described next.

Crucial to this work is the *link line-of-sight condition*. We focus on scenarios where an UWB tag ranging with one or more device(s) is worn on the chest by a person as a necklace of sorts, common in several human-centric UWB applications (e.g., [1, 5, 6]). We reproduce this situation by attaching devices at 1.35 m height to wooden supports (Figure 3a) and placing one of the authors (1.74 m height, 64 kg weight) with the chest touching one of them. This solution closely mimics the real situation while ensuring repeatability, preventing unwanted movements, and simplifying experiment execution.

We consider three arrangements yielding different link conditions. In the first one, the subject stands in front of one device, fully occluding the link and therefore yielding HNLOS, the focus of our study. In the second one, the subject is positioned behind the device, which therefore is in LOS. However, the human body touching the device may still have an impact on ranging and detection; we call this situation, often neglected in the literature, human LOS (HLOS). Finally, our third setup removes the human body altogether, yielding a pure LOS condition serving as comparison baseline.

We also study how the *TWR role of the occluded device* affects ranging and detection by distinguishing the case where the subject is placed next to the initiator (I-SHIELDED) or the responder (R-SHIELDED), as shown in Figure 3b.

Both dimensions above are evaluated in a *deployment setup* that, as mentioned earlier, depends on the application scenario. We consider the paradigmatic cases that inspired our work (§I) and distinguish (Figure 3c) between the case where the devices of a link are both placed on PEOPLE at the same height, as in proximity-based applications [1], and the one where the non-occluded device is installed on the CEILING, a common placement for the anchors of UWB systems tracking users [5]. In both cases we study, wherever possible, a different *distance* between devices, $d \in \{1.5, 3, 10, 20, 30\}$ m.

All our experiments exploit a single link with two UWB devices, a simple setup allowing us to explore many combinations with good repeatability and limited effort. We deploy the link in two *environments* with different characteristics: an office CORRIDOR and the HALL of our building. In the former, the walls separated by a narrow width (2.5 m) and the low ceiling (2.6 m) increase the likelihood of multipath effects that, as noticed (§III), play a role in NLOS conditions. The wider area (52×8 m^2) and higher ceiling (3 m) of the latter is less prone to these effects, yielding a valid comparison. Due

TABLE I
EXPERIMENTAL SETTINGS.

line-of-sight condition of the link	LOS, HLOS, HNLOS
TWR role of the occluded device	R-SHIELDED, I-SHIELDED
distance (m)	1.5, 3, 10, 20, 30
deployment setup	PEOPLE, CEILING
environment	CORRIDOR, HALL
radio configuration	cLOS, cMIXED, cNLOS, cLOS_{1024}
RF channel	2, 4, 5

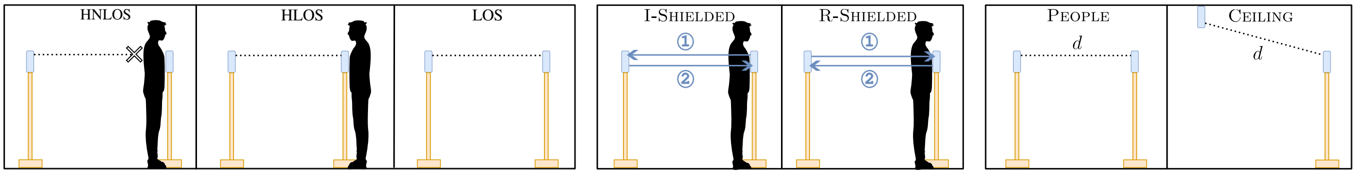

(a) Line-of-sight condition of the link. (b) TWR role of the occluded device. (c) Deployment setup.

Fig. 3. Experimental settings.

to space limits, in §VI–§VII we first report about CORRIDOR, followed by the salient differences w.r.t. HALL, if any.

As for UWB, we experiment with the four *radio optimizations* we identified (§IV) and three *RF channels* (CH). CH5 is the one recommended by the manufacturer for the DW1001 boards we use. We explore also CH2 and 4 as they are popular choices for the DW1000 chip on other boards given they both have lower center frequency (hence path loss) than CH5, and CH4 has also wider bandwidth (hence higher range). This choice actually enabled interesting insights, discussed later.

Our experiments sweep all parameters in Table I. For each of the 720 combinations, we perform a dedicated experiment of 500 successful rangings (TWR executions) for which we acquire individual distance estimates along with radio diagnostics necessary to compute the link indicators (§IV).

VI. RANGING RELIABILITY AND ACCURACY

Metrics. Human occlusion can completely prevent communication, thus ranging. Therefore, we report about its *reliability* in terms of TWR exchanges correctly executed vs. performed, quantified as the packet reception rate (PRR) of the RESPONSE packet at the initiator. Then, we quantify *ranging errors* by computing the difference between distances acquired with the human subject in a given experimental setting vs. the median distance estimated *in the same setting* but without the subject, i.e., in LOS conditions. By using the latter as a baseline, we focus solely on the impact of the human body (notably, timestamp errors e_I, e_R, §III), as everything else remains the same. We report the median (μ) and 90^{th} percentile (90^{th}) of the error defined above.

Reliability. In all combinations tested, packet losses occur predominantly at the longest distance tested of $d = 30$ m.

Overall, CH2 and 4 are the most reliable. cLOS and cMIXED achieve perfect reliability regardless of the link line-of-sight condition; this is often achieved also by the majority of combinations with cNLOS and cLOS$_{1024}$ whose lowest PRR are, respectively, 98.4% (HNLOS) and 99.2% (HLOS).

Instead, CH5 is significantly less reliable especially over long distances, due to its higher frequency and hence path loss. In LOS, no configuration systematically achieves perfect reliability, but $PRR \geq 99\%$ for cLOS and cMIXED, and $PRR \geq 90.3\%$ for cNLOS, the most unreliable. In HLOS, all configurations achieve similar reliability, except for cNLOS whose PRR degrades to 64.9% (CEILING). Instead, in HNLOS reliability degrades across all configurations, albeit without clear trends. cLOS yields the lowest $PRR = 32.5\%$, and only slightly higher (36.3%) for its cLOS$_{1024}$ variant.

Spurious estimates. Packet losses aside, another threat to ranging are grossly incorrect or even nonsensical estimates.

A large distance overestimate can be caused by the delay incurred by the signal (hence its first path) when occluded by the human body in HNLOS (Figure 2). Instead, an underestimate is more likely from optimizations with a low noise multiplier, cMIXED and especially cNLOS (§IV). An earlier noise peak may be detected in the CIR instead of the signal one, yielding an underestimate or, depending on the conditions, even a nonsensical negative distance. The latter is clearly unusable and results in wasted resources; however, it can be easily detected and filtered out, unlike a generic underestimate.

These expectations are confirmed by our results, where we focus on errors of at least ± 1 m. Overestimates appear for all optimizations only in HNLOS and are largest with $d \geq 20$ m; CH5 performs the worst, with nearly all rangings at $d = 30$ m

TABLE II

SPURIOUS RESULTS IN CNLOS (CORRIDOR). EACH VALUE (PERCENTAGE) AGGREGATES THE 2 TYPES OF TWR OCCLUSION AND ALL 5 DISTANCES CONSIDERED (5000 RANGING ESTIMATES). UNDER- AND OVER-ESTIMATES PERCENTAGES CONSIDER ERRORS GREATER THAN ± 1 M AND ARE COMPUTED AFTER REMOVING NEGATIVE ESTIMATES.

		PEOPLE			CEILING		
CH	Outcome	LOS	HLOS	HNLOS	LOS	HLOS	HNLOS
2	Negative	2.7	6.9	0.8	4.4	4.2	0.6
	Underestimate	2.0	2.8	0.0	0.1	0.2	0.2
	Overestimate	0.0	0.0	8.1	0.0	0.0	16.3
4	Negative	13.8	18.2	13.7	3.4	14.0	2.1
	Underestimate	1.0	2.4	3.6	2.0	7.6	0.6
	Overestimate	0.0	0.0	3.3	0.0	0.0	2.8
5	Negative	1.8	1.4	1.1	0.6	4.0	3.8
	Underestimate	0.9	3.6	0.1	0.0	0.6	0.0
	Overestimate	0.0	0.0	23.6	0.0	0.0	31.6

TABLE III

SPURIOUS RESULTS IN CNLOS (HALL), $d \leq 10$ M.

		PEOPLE			CEILING		
CH	Outcome	LOS	HLOS	HNLOS	LOS	HLOS	HNLOS
2	Negative	0.2	5.2	7.6	0.8	5.0	20.2
	Underestimate	0.0	0.0	0.0	0.0	0.0	0.0
	Overestimate	0.0	0.0	0.2	0.0	0.0	0.0
4	Negative	33.4	26.8	35.7	26.4	23.6	48.2
	Underestimate	1.8	0.8	0.0	8.8	1.2	0.0
	Overestimate	0.0	0.0	0.0	0.0	0.0	0.0
5	Negative	3.2	14.3	28.0	38.5	8.8	0.6
	Underestimate	0.0	0.1	0.0	0.0	0.0	0.0
	Overestimate	0.0	0.0	13.6	0.0	0.0	17.3

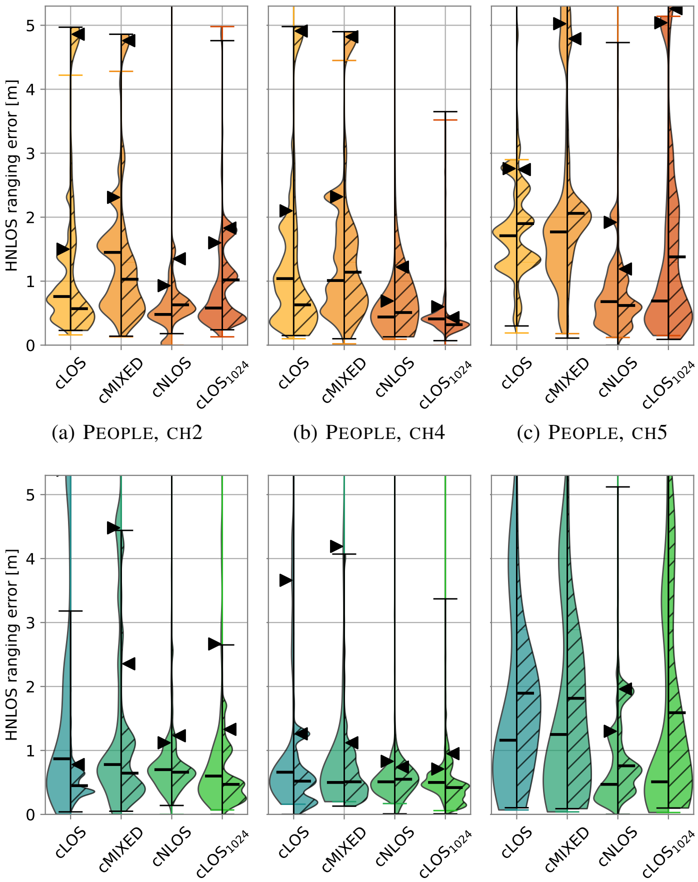

(a) PEOPLE, CH2 (b) PEOPLE, CH4 (c) PEOPLE, CH5

(d) CEILING, CH2 (e) CEILING, CH4 (f) CEILING, CH5

Fig. 4. CORRIDOR: Ranging errors in HNLOS. Violins show R-SHIELDED (left) and I-SHIELDED (right); whiskers show the extremes (dark for I-SHIELDED); inner ticks show the median μ; triangles show the 90^{th} percentile.

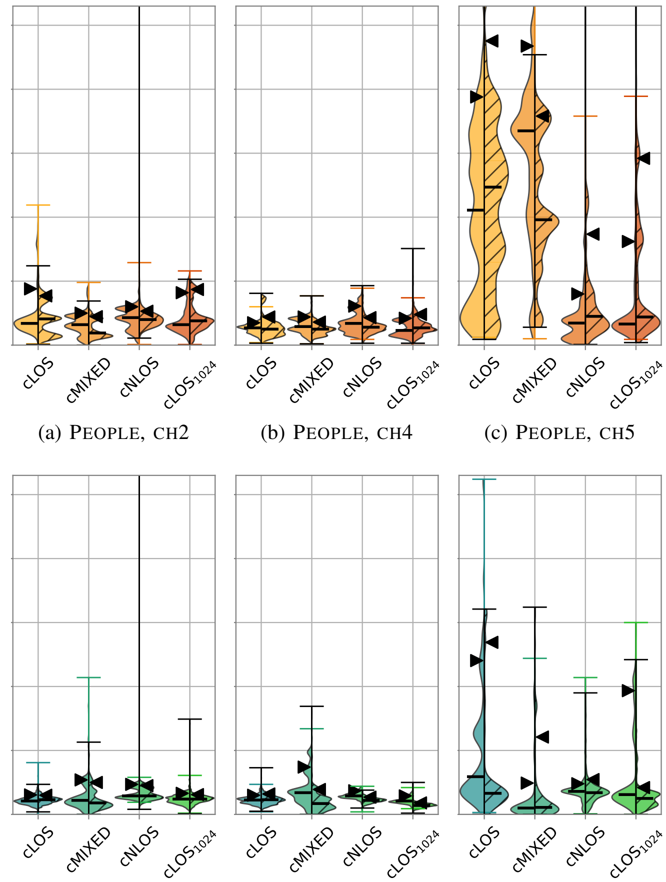

(a) PEOPLE, CH2 (b) PEOPLE, CH4 (c) PEOPLE, CH5

(d) CEILING, CH2 (e) CEILING, CH4 (f) CEILING, CH5

Fig. 5. HALL: Ranging errors in HNLOS. The figure elements have the same meaning of Figure 4. Only distances $d \leq 10$ m are considered, as not all channels operate reliably at longer distances.

affected by ≥ 1 m error. Overestimates at $d = 30$ m are less frequent with cNLOS: 31–92% depending on the setting.

This optimization deserves further attention (Table II) as it is the only one yielding underestimates, due to its lowest noise multiplier, and the manufacturer reports that it may yield spurious estimates even in LOS conditions [21]. Our results quantify this aspect; negative estimates appear in all link conditions, although they tend to be higher in HLOS. Further, CH4 is the most affected, with negative estimates accounting for nearly 20% of the total in some cases. On the other hand, CH5 is by far the most affected by overestimates.

Hereafter, the results for cNLOS are reported after discarding the negative estimates, as any practical system would. Nevertheless, although this optimization achieves better accuracy, as discussed next, this comes at the cost of a high probability of ranging failure or nonsensical estimates, as shown above.

LOS vs. HLOS: Does it matter to ranging estimates? All optimizations perform well in LOS conditions. As we use the LOS median as a comparison baseline, what needs to be assessed is the *precision* of results. The median absolute deviation aggregated across distances is very low, $\leq$2 cm. The 90^{th} of the deviation from the median is very small; the worst ones are only 8 cm (CH5, cLOS_{1024}) and 6 cm (CH2, cLOS).

The question is whether the presence of the body behind the device in HLOS conditions affects accuracy. The answer is generally negative; except in few cases affected by cNLOS spurious estimates, we do not observe significant differences w.r.t. LOS. By comparing results aggregated across all distances and considering the LOS median as ground truth, the HLOS median error is $\leq$3 cm regardless of all other settings (Table I). The two link conditions also yield a similar dispersion, with an increase $\leq$9 cm of the 90^{th} error percentile.

Reducing errors in HNLOS: Which radio configuration? On the other hand, in HNLOS the presence of a human occlusion on the link induces significant ranging errors (Figure 4).

In terms of channels, CH5 yields the lowest accuracy. The error distributions for the various optimizations in both PEOPLE and CEILING (Figure 4c and 4f) are significantly longer-tailed w.r.t. other channels; consequently, μ and 90^{th} are also significantly higher. For instance, cLOS_{1024} in CH5 (I-SHIELDED) achieves $90^{th} = 9.35$ m, against 1.33 m (CH2) and 0.95 m (CH4). The differences between the other two channels are less evident, although CH4 performs slightly better.

As for radio optimizations, cLOS and cMIXED consistently yield the worst accuracy across channels, with very long tails. cMIXED achieves $90^{th} \geq 1$ m, often much higher for both

R-SHIELDED and I-SHIELDED. In CH5, these optimizations achieve $\mu \geq$1.15 m. Interestingly, our variant cLOS$_{1024}$ performs significantly better, especially in CH4 where it achieves a sub-meter 90^{th}. In this configuration, it is even slightly better than cNLOS, which otherwise is the best optimization across channels, type of TWR occlusion, and deployment setup; it always ensures sub-meter μ and $90^{th} < 2$ m. Nonetheless, except for CH5, where the difference in accuracy w.r.t. the other optimizations is remarkable, the choice of cNLOS can be hardly justified given the low reliability discussed earlier.

Is ranging error affected by distance? The long-tailed error distributions for HNLOS (Figure 4) are mostly ascribed to links of length $d \geq 20$ m, regardless of radio configuration, type of TWR occlusion, and deployment setup (Figure 6).

This is not the case in LOS or HLOS; in HNLOS, the signal attenuation induced by human occlusion makes long-range communication more challenging, often resulting in overestimation, as mentioned.

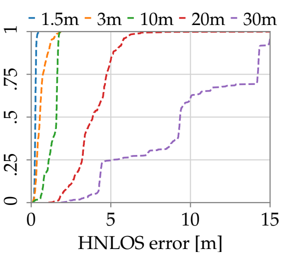

Fig. 6. HNLOS error vs. distance (CDF) in CH5, CEILING, cLOS$_{1024}$, I-SHIELDED.

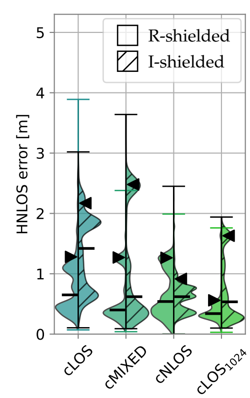

Fig. 7. CH5, CEILING, $d \leq 10$ m.

All optimizations improve drastically when $d \leq 10$ m, across channels. In CH5 (Figure 7) the 90^{th} achieved by, e.g., cLOS$_{1024}$ for R-SHIELDED improves from 8.31 m to 0.56 m (CEILING) and from 5.04 m to 2.01 m (PEOPLE, not shown). In CH4 the 90^{th} of the best optimization, cLOS$_{1024}$, is within 0.4–0.68 m across settings. Interestingly, on the same short distances, cLOS accuracy is similar in CEILING, $90^{th} < 1$ m; in PEOPLE, improvements are less remarkable, $90^{th} \approx 2$ m. In CH2, cLOS$_{1024}$ has 90^{th} within 0.94–1.1 m.

Deployments and occlusions: Do they matter? From the full experimental campaign in CORRIDOR, no difference between deployments (PEOPLE vs. CEILING) can be drawn. However, when considering $d \leq 10$ m, CH2 and CH4 show marginally better accuracy in CEILING, possibly due to a less marked HNLOS due to the relative position of the device on the ceiling and the occluded one. As for the type of TWR occlusion, no consistent trend is found. Although we observe that the 90^{th} of R-SHIELDED is significantly higher in CEILING and, on the contrary, the one of I-SHIELDED is higher in PEOPLE, we consider this an effect caused by the specific environment. Indeed, these observations only hold at $d \geq 20$ m, where the overestimates affecting 90^{th} are likely the result of reflections. Further, they are not confirmed in HALL, the other environment we consider and the focus of the rest of this section.

What is the impact of the environment? We now report the salient results acquired by repeating the same experiments in HALL. First, we observe that the HNLOS reliability at high distances decreases for all channels w.r.t. CORRIDOR, a somewhat counterintuitive result given that the latter is affected by multipath (§V). The decrease is most evident in CH5, where links with $d = 20$ already yield $PRR \approx 0$ across all settings, except when using cLOS$_{1024}$ ($PRR > 21.1\%$). At the other extreme, CH4 is the only channel that can be used reliably even at $d = 30$ m, with $PRR \geq 88.5\%$. CH2 performs in between, since it has lower frequency (hence path loss) than CH5, but narrower bandwidth than CH4. The decrease in PRR is explained by the lack of strong signal reflections in HALL, instead present in the narrower CORRIDOR. These are normally a threat to ranging accuracy, yet in HNLOS they improve PRR by contributing to the signal power received [21] and facilitating preamble detection, the first step in packet RX.

As for ranging accuracy, our main findings are confirmed; as in CORRIDOR, we observe no relevant difference between LOS and HLOS. Underestimates, including negative ones, appear only for cNLOS, and overestimates only in HNLOS.

Still some differences emerge. As mentioned, ranging up to 30 m is reliable only in CH4; further, its accuracy degrades, more markedly than in CORRIDOR. As expected, this affects mainly cNLOS, but also cLOS and cMIXED, with 90^{th} to several meters in some settings. cLOS$_{1024}$ is less affected, achieving acceptable accuracy across all settings ($90^{th} < 1.18$ m). Due to the decrease in PRR on all other channels, hereafter we limit our comparison with CORRIDOR to $d \leq 10$ m.

HNLOS errors in HALL are shown in Figure 5. In CH5, only cNLOS and cLOS$_{1024}$ yield accurate ranging. The median error is $\mu < 0.45$ m regardless of the setting, but 90^{th} is lower in cNLOS w.r.t. cLOS$_{1024}$: 1.74 m vs. 2.92 m (PEOPLE) and 0.55 m vs 1.93 m (CEILING). Overall, cNLOS is slightly more accurate in CH5; yet, it is also significantly less reliable than in CORRIDOR, due to increased negative estimates (Table III).

These affect cNLOS also in CH2 and CH4, where it achieves accuracy comparable to cLOS$_{1024}$ and cLOS; we focus on these as they are not affected by the same problem, yet achieve similar accuracy, outperforming cMIXED. As observed in CORRIDOR, accuracy is slightly higher in CEILING, with 90^{th} within 0.18–0.33 m. As for PEOPLE, CH4 yields slightly better 90^{th} (0.35–0.48 m) than CH2 (0.5–0.88 m). Taking results together, and comparing to those of CORRIDOR at the same distances, 90^{th} in CH2 and 4 are always similar or lower in HALL, where reflections are not as strong.

These findings complement those in CORRIDOR, enabling us to distill guidelines on how to configure the radio for ranging (§VIII-A). Nevertheless, their practical application hinges on the knowledge of link line-of-sight condition, guiding the selection of an appropriate configuration. Unfortunately, a configuration yielding reliable and accurate ranging in HNLOS may not necessarily yield also accurate HNLOS detection, or vice versa. We analyze this crucial aspect in the next section.

VII. DETECTING LINK LINE-OF-SIGHT CONDITIONS

Metrics. For both radio indicators, the manufacturer states the values yielding high-confidence classification into LOS

TABLE IV
CORRIDOR: HIGH-CONFIDENCE LINK ESTIMATES AND THEIR ACCURACY AS HC (TPR).

CH	OPT	PEOPLE CL	PEOPLE CL^*	PEOPLE PD	CEILING CL	CEILING CL^*	CEILING PD
				LOS			
2	cLOS	100 (100)	100 (99.8)	100 (100)	84.0 (99.8)	84.0 (100)	88.2 (98.8)
	cMIXED	99.8 (99.4)	99.8 (100)	100 (100)	80.5 (99.9)	80.5 (100)	84.2 (98.6)
	cNLOS	99.4 (47.9)	99.3 (97.6)	90.3 (97.3)	95.2 (50.0)	79.3 (96.1)	53.4 (94.8)
	cLOS$_{1024}$	99.9 (99.9)	99.9 (100)	100 (100)	80.3 (99.0)	80.2 (99.1)	83.9 (98.0)
4	cLOS	98.4 (99.8)	98.3 (100)	100 (100)	99.2 (99.5)	99.2 (100)	99.6 (100)
	cMIXED	99.7 (98.1)	99.7 (100)	100 (100)	99.1 (99.4)	99.1 (100)	99.6 (100)
	cNLOS	99.7 (28.7)	99.6 (92.7)	94.8 (92.6)	98.8 (18.8)	95.8 (96.9)	72.5 (96.1)
	cLOS$_{1024}$	99.8 (99.6)	99.8 (100)	99.9 (99.9)	99.0 (99.4)	99.0 (100)	99.3 (100)
5	cLOS	89.5 (43.8)	88.4 (43.3)	64.6 (70.0)	93.1 (78.7)	93.1 (78.9)	59.8 (100)
	cMIXED	88.6 (65.8)	88.4 (65.8)	68.6 (70.8)	100 (83.2)	100 (83.6)	70.0 (100)
	cNLOS	90.2 (34.4)	85.8 (69.2)	42.9 (43.4)	99.2 (34.9)	99.1 (88.7)	50.3 (99.8)
	cLOS$_{1024}$	83.8 (74.2)	82.4 (76.1)	54.9 (76.3)	100 (88.5)	100 (89.2)	46.4 (100)
				HLOS			
2	cLOS	99.8 (100)	99.8 (100)	100 (100)	83.1 (99.3)	83.1 (99.4)	89.4 (99.3)
	cMIXED	98.9 (99.1)	98.9 (100)	100 (100)	79.5 (86.2)	79.1 (88.2)	75.8 (98.3)
	cNLOS	99.4 (63.1)	99.1 (95.9)	85.3 (95.7)	90.4 (48.3)	73.3 (93.9)	68.3 (93.0)
	cLOS$_{1024}$	95.8 (99.9)	95.8 (100)	99.7 (100)	80.5 (98.0)	80.4 (99.9)	87.5 (94.9)
4	cLOS	99.7 (98.3)	99.7 (100)	100 (100)	99.3 (98.1)	99.3 (100)	100 (100)
	cMIXED	98.4 (94.1)	98.4 (100)	100 (100)	97.7 (93.1)	97.7 (99.0)	97.6 (100)
	cNLOS	99.8 (20.8)	99.2 (87.6)	97.6 (87.4)	99.5 (16.6)	96.7 (82.2)	79.4 (78.5)
	cLOS$_{1024}$	97.2 (99.9)	97.1 (100)	99.9 (99.9)	98.9 (92.6)	98.8 (99.9)	98.7 (99.9)
5	cLOS	73.9 (35.5)	73.2 (35.9)	63.4 (38.5)	95.0 (69.4)	94.7 (70.1)	89.1 (79.7)
	cMIXED	78.1 (53.1)	76.8 (54.7)	51.9 (65.7)	92.9 (74.8)	92.6 (75.3)	81.1 (78.8)
	cNLOS	90.9 (24.8)	86.3 (42.8)	55.1 (31.9)	99.1 (40.4)	97.2 (68.2)	45.2 (71.0)
	cLOS$_{1024}$	81.4 (54.9)	80.2 (56.2)	70.5 (54.5)	81.5 (63.9)	81.0 (65.1)	57.5 (63.8)
				HNLOS			
2	cLOS	99.6 (100)	99.4 (96.2)	94.8 (96.0)	98.9 (99.6)	98.4 (99.5)	95.0 (98.8)
	cMIXED	99.0 (99.5)	98.7 (92.8)	93.6 (92.4)	99.9 (99.4)	99.8 (98.8)	93.5 (99.0)
	cNLOS	99.8 (94.3)	99.8 (91.8)	93.5 (96.6)	100 (99.1)	98.8 (98.6)	97.5 (99.9)
	cLOS$_{1024}$	94.1 (99.9)	93.4 (99.9)	97.9 (100)	99.8 (100)	99.8 (100)	99.9 (99.9)
4	cLOS	98.3 (100)	86.9 (95.4)	90.1 (95.4)	99.9 (92.5)	99.8 (92.3)	92.2 (98.4)
	cMIXED	99.2 (99.1)	93.0 (88.6)	87.2 (89.2)	99.0 (99.7)	98.0 (99.5)	98.1 (97.8)
	cNLOS	100 (100)	100 (99.9)	100 (99.9)	100 (99.9)	100 (94.3)	92.4 (99.6)
	cLOS$_{1024}$	97.3 (99.9)	96.6 (99.8)	99.1 (99.8)	99.9 (99.6)	99.9 (99.6)	99.4 (100)
5	cLOS	93.2 (88.8)	88.6 (74.4)	89.0 (77.8)	90.0 (99.8)	83.8 (99.2)	80.4 (96.3)
	cMIXED	98.2 (98.8)	86.1 (87.0)	84.9 (90.1)	94.7 (100)	84.2 (99.5)	83.9 (93.1)
	cNLOS	95.9 (99.8)	90.9 (99.7)	98.5 (99.9)	100 (100)	100 (99.9)	96.0 (99.7)
	cLOS$_{1024}$	99.8 (99.5)	93.9 (91.7)	89.4 (92.4)	99.5 (99.9)	94.6 (98.7)	98.4 (98.7)

TABLE V
HALL: HIGH-CONFIDENCE LINK ESTIMATES AND THEIR ACCURACY AS HC (TPR), ONLY FOR RELIABLE LINKS $d \leq 10$ M.

CH	OPT	PEOPLE CL	PEOPLE CL^*	PEOPLE PD	CEILING CL	CEILING CL^*	CEILING PD
				LOS			
2	cLOS	99.8 (100)	99.8 (99.4)	100 (100)	82.0 (93.9)	82.0 (100)	95.8 (100)
	cMIXED	90.4 (67.8)	88.9 (82.3)	92.1 (100)	84.8 (99.8)	84.7 (100)	99.7 (100)
	cNLOS	99.4 (93.0)	99.4 (99.6)	95.2 (100)	97.0 (49.3)	91.6 (99.7)	80.7 (99.6)
	cLOS$_{1024}$	100 (100)	100 (100)	100 (100)	59.6 (99.0)	59.2 (100)	83.8 (100)
4	cLOS	100 (100)	100 (100)	100 (100)	99.9 (97.5)	99.8 (100)	100 (100)
	cMIXED	100 (93.9)	100 (100)	100 (100)	99.2 (100)	99.2 (100)	100 (100)
	cNLOS	100 (26.3)	100 (78.9)	99.8 (78.9)	97.8 (30.9)	97.2 (77.6)	99.4 (78.1)
	cLOS$_{1024}$	100 (100)	100 (100)	99.9 (100)	100 (99.8)	100 (100)	100 (100)
5	cLOS	100 (99.4)	100 (100)	100 (100)	100 (74.9)	100 (75.0)	93.8 (100)
	cMIXED	100 (97.2)	100 (97.7)	66.7 (100)	100 (99.6)	100 (100)	100 (100)
	cNLOS	99.9 (62.8)	99.9 (97.1)	95.3 (97.0)	100 (62.8)	100 (78.2)	100 (78.2)
	cLOS$_{1024}$	97.0 (99.5)	97.0 (100)	66.7 (100)	100 (98.8)	100 (100)	100 (100)
				HLOS			
2	cLOS	99.6 (99.7)	99.6 (100)	100 (100)	78.4 (99.0)	78.4 (99.9)	88.9 (91.9)
	cMIXED	95.4 (84.9)	95.3 (90.2)	88.5 (97.7)	96.3 (99.5)	96.3 (99.7)	98.9 (99.1)
	cNLOS	98.7 (83.6)	98.5 (97.1)	79.7 (97.7)	96.1 (71.2)	92.3 (97.8)	85.9 (97.3)
	cLOS$_{1024}$	94.5 (98.5)	94.5 (98.6)	86.6 (99.3)	88.2 (96.1)	88.2 (96.1)	86.7 (97.8)
4	cLOS	99.6 (99.9)	99.6 (99.9)	100 (100)	98.7 (99.2)	98.7 (100)	98.8 (100)
	cMIXED	99.8 (87.1)	99.8 (99.0)	99.0 (100)	98.3 (96.1)	98.3 (100)	100 (100)
	cNLOS	99.8 (23.9)	99.7 (75.3)	94.7 (74.4)	99.6 (31.5)	99.2 (80.6)	95.6 (81.0)
	cLOS$_{1024}$	99.8 (97.5)	99.8 (97.7)	98.1 (99.9)	99.5 (97.6)	99.4 (99.2)	98.8 (100)
5	cLOS	97.3 (88.4)	97.3 (88.6)	78.4 (96.9)	98.9 (68.1)	98.9 (77.2)	92.6 (99.4)
	cMIXED	96.6 (78.6)	96.6 (79.4)	77.9 (84.2)	99.4 (81.3)	99.3 (85.8)	90.2 (98.2)
	cNLOS	97.9 (51.9)	97.0 (74.1)	71.9 (77.7)	99.7 (74.0)	99.5 (92.7)	96.8 (95.5)
	cLOS$_{1024}$	87.6 (76.0)	87.6 (76.6)	61.5 (83.9)	98.9 (92.1)	98.8 (92.5)	90.6 (97.2)
				HNLOS			
2	cLOS	100 (100)	100 (100)	99.6 (100)	100 (92.8)	100 (92.6)	76.1 (96.3)
	cMIXED	100 (98.1)	100 (98.1)	93.5 (100)	100 (99.1)	100 (99.0)	81.5 (98.9)
	cNLOS	100 (99.9)	100 (99.8)	96.7 (99.9)	100 (100)	100 (96.2)	80.5 (99.5)
	cLOS$_{1024}$	99.9 (99.2)	99.9 (99.2)	97.9 (99.9)	100 (97.8)	100 (97.8)	84.2 (98.3)
4	cLOS	100 (98.4)	100 (98.4)	92.2 (99.3)	100 (93.8)	100 (93.8)	63.1 (96.0)
	cMIXED	100 (97.4)	100 (97.4)	90.6 (100)	100 (87.6)	100 (87.6)	66.2 (88.5)
	cNLOS	100 (99.9)	100 (99.6)	94.0 (100)	100 (100)	100 (96.8)	69.6 (97.4)
	cLOS$_{1024}$	100 (100)	100 (100)	96.7 (99.9)	100 (97.4)	100 (97.4)	94.8 (99.4)
5	cLOS	100 (100)	99.0 (83.7)	92.1 (88.9)	98.8 (100)	93.8 (99.6)	98.7 (100)
	cMIXED	100 (100)	99.9 (96.9)	96.2 (96.9)	100 (100)	98.0 (100)	99.6 (100)
	cNLOS	100 (100)	100 (100)	99.9 (99.9)	100 (100)	100 (99.9)	99.8 (100)
	cLOS$_{1024}$	100 (100)	100 (99.6)	99.4 (99.9)	100 (100)	99.6 (100)	100 (99.9)

($CL = 1$, $PD < 6$) and NLOS ($CL = 0$, $PD > 10$), with intermediate results considered uncertain (§IV). Accordingly, we report *i)* the fraction of high-confidence (HC) estimates, matching either condition above, in percentage over the total number of successful rounds, and *ii)* their classification accuracy via the true positive rate $TPR = \frac{TP}{TP+FN}$.

Can the radio correctly detect line-of-sight conditions? In short, Table IV shows that the answer is positive; HC estimates are the vast majority and their TPR is typically very high. Crucially, this means that the indicators returned by the radio can be used *as is* without further calibration or processing required, e.g., by thresholds or energy-hungry machine learning approaches, respectively.

In CH4, the fraction of HC values is >98.3% in LOS and >87.2% in HNLOS, regardless of the indicator and across all optimizations except cNLOS. The difference between CL and PD is small, within few percent. HC in CH2 exhibits a similar trend, although slightly lower in CEILING for LOS (>80.3%). Equally important, these HC estimates yield highly accurate classification in both channels; TPR is often nearly perfect, rarely <95% overall. Again, this holds for all optimizations except cNLOS, notably including our variant cLOS$_{1024}$, which performs well both in CH4 (>99.4%) and CH2 (>98%).

cNLOS and CH5 deserve a separate discussion, as they exhibit marked differences w.r.t. indicators and are overall less dependable. Using cNLOS, the HC estimates returned by CL are mostly correct in HNLOS, but frequently incorrect in LOS, with $TPR < 50\%$. As with ranging, the culprit is the use of the lowest noise multiplier, causing the radio to mistake noise for an undetected first path; this yields $LUEP > 0$ which directly translates to the HC value $CL = 0$ (§IV), misclassifying the link as HNLOS. As for PD, the fraction of HC estimates in LOS is significantly lower, especially in CEILING, but it is very accurate at least in CH2 and 4 ($TPR > 92.6\%$). In the same channels, HNLOS detection is both high-confidence and accurate ($HC > 92.3\%$, $TPR > 96.5\%$). Interestingly, the combination of the two enables correct detection: any link not HC in HNLOS is, dually, likely LOS (Table IV).

Concerning CH5, both the fraction of HC estimates and their TPR is drastically reduced w.r.t. other channels. Again, CL often mistakes LOS for HNLOS, this time regardless of the optimization, and PD yields fewer HC estimates. Moreover, unlike the other channels, the TPR in LOS is high in CEILING but low in PEOPLE for PD, limiting its applicability.

Is HLOS correctly detected as LOS? The body behind the device in HLOS does not affect significantly ranging accuracy (§VI). To be useful to applications, we therefore expect the indicators to report HLOS links as LOS. Table IV shows that this is indeed the case, with high confidence and accuracy, except for CH5 and cNLOS. Both are nonetheless already problematic in LOS and therefore disregarded hereafter.

In CH4, HC estimates are >97.2% (HLOS) vs. >98.3% (LOS) across both indicators and all optimizations. Similar small differences occur in CH2 including in CEILING where, like in LOS, HC estimates are generally lower. Detection accuracy is also similar to LOS conditions, with TPR typically very close to 100%; the only exception is cMIXED, from a few higher differences (up to 13.8% in CH2) are observed.

Improving CL-based detection in cNLOS. In HNLOS, the optimization yielding best ranging accuracy is cNLOS. In some applications, this may be enough motivation to use it, despite being plagued by negative estimates. However, although CL correctly classifies HNLOS conditions when used with cNLOS, it *does not* yield accurate (H)LOS detection, regardless of the settings. As noted, the culprit is the interplay of the LDE noise threshold with $LUEP$ component in CL. Once this is removed in our variant CL^* (§IV), accuracy in LOS conditions improves substantially, with minimal impact in HNLOS; the largest improvement is in CH4 (CEILING) where TPR increases from an unacceptable 18.8% to 96.9%, becoming even more accurate (and HC) than PD. Similar improvements occur for HLOS, albeit slightly less prominent.

Distance, deployments, and occlusions: Do they matter? Distances and deployments have a significantly lower impact for detection than the channel frequency. In CH4, their effect is essentially negligible. At the other extreme, in CH5 the general higher variability of results prevents us from highlighting any clear trend. Therefore, we focus on CH2, offering insights contributing to the overall interpretation of our results.

Figure 8 shows that the limited confidence in (H)LOS link classification for both indicators in CEILING with CH2 (Table IV) is actually caused by their unreliable operation at $d = 30$ m in this setting. At shorter distances, differences between deployments are less marked and HC estimates are the majority. An exception to the above is the combination of cNLOS and PD, which for $d \leq 3$ m yields significantly fewer HC estimates especially in CEILING (Figure 8h); instead, CL^* performs significantly better (Figure 8d). These latter observations actually generalize to all channels.

As for type of TWR occlusion, no clear trend emerges, similar to ranging (§VI). In HLOS conditions, differences are more relevant in CEILING and CH5, where I-SHIELDED often induces lower TPR. Instead, in HNLOS PEOPLE is more sensitive than CEILING to the type of TWR occlusion, whose detrimental effect nonetheless varies according to the combination of channel and optimization. Finally, as in ranging, these trends are not confirmed in HALL, discussed next.

What is the impact of the environment? Table V shows HC estimates and related TPR in HALL, limited to $d \leq 10$ m as ranging is not always reliable over longer distances (§VI). Our main finding from CORRIDOR is confirmed: radio indicators generally yield high-confidence, accurate estimates of line-of-sight conditions, often with even higher HC and/or TPR.

In CH2 and CH4, HC estimates are the vast majority and very accurate across link conditions and optimizations, except for cNLOS. CH2 has a lower fraction of HC for LOS in CEILING, as in CORRIDOR; TPR is similar in the two channels. Notably, cLOS$_{1024}$, our proposed optimization, always achieves a detection accuracy $> 96\%$, unlike other optimizations for which TPR degrades in some settings. Moreover, when exploited with CL, cLOS$_{1024}$ detects HNLOS conditions with $HC > 99.9\%$; uncertain estimates can therefore be reliably considered as LOS. Interestingly, cLOS$_{1024}$ accuracy remains high even at $d \geq 20$ m in CH4 (not shown): $TPR > 97.5\%$ across all indicators, settings, and line-of-sight conditions. As for HC, its value degrades as distance increases in some (H)LOS settings (e.g., -36% in CEILING, LOS), but remains $> 97.6\%$ in HNLOS. At the other extreme, confirming our observations in CORRIDOR, cNLOS is the most unreliable optimization, especially with CL; however, CL^* drastically improves its LOS detection, yielding a TPR similar to PD and often a higher HC. Nonetheless, (H)LOS detection accuracy with both indicators in CH4 remains significantly lower ($\sim$20%) in cNLOS w.r.t. other optimizations.

In CH5, differences w.r.t. CORRIDOR are more marked. In HNLOS, the HC and TPR of both CL and PD is significantly higher, approaching or even exceeding what achieved in the other channels. Similar considerations hold also for LOS. Significant improvements w.r.t. to CORRIDOR are also registered in HLOS, although TPR is only seldom >90%, especially for CL, for which we verified that the human body reduces M_C and increases $PrNLOS$ even without an occlusion (§IV). As for PD, apart when exploited in combination with cNLOS, it achieves perfect accuracy in LOS and $TPR > 83.9\%$ in HLOS. Finally, it is worth noting that the improvements observed for CH5 in HALL vs. CORRIDOR are not a consequence of the shorter distances considered in the former; improvements persist, sometimes even more pronounced, when comparing against the latter with $d \leq 10$ m.

VIII. DISCUSSION

Our study is experimental, therefore inevitably biased by the conditions in which it has been carried out.

We focused on the scenario where the UWB tag is worn on the chest, motivated by its common use in several applications, and considered only this single human occlusion. However, in proximity detection applications [1] (PEOPLE), distance may be estimated between two people even when they are turning their back to each other. More generally, an arbitrary number of people may be present on a link, at different distances and possibly with partial occlusions. Also, people have different body characteristics, possibly yielding slightly different HNLOS conditions. These aspects depend on the specific deployment and are hard to characterize in general.

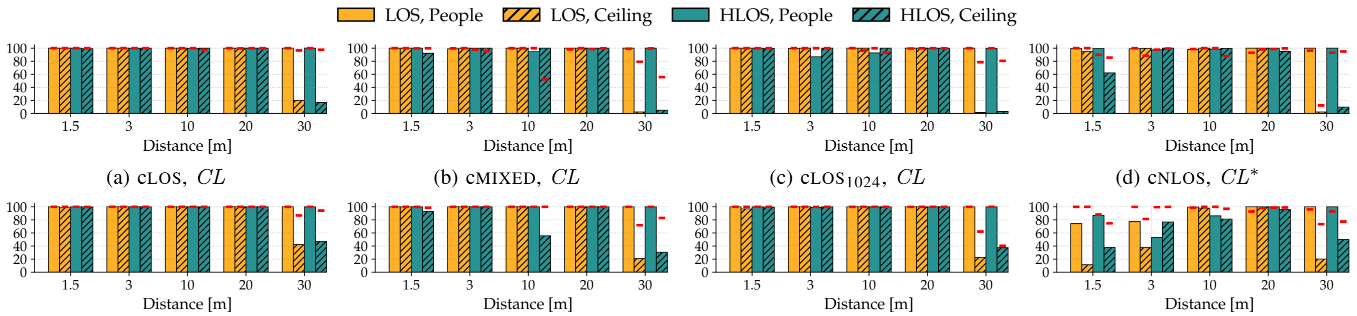

(a) cLOS, CL (b) cMIXED, CL (c) cLOS$_{1024}$, CL (d) cNLOS, CL^*

(e) cLOS, PD (f) cMIXED, PD (g) cLOS$_{1024}$, PD (h) cNLOS, PD

Fig. 8. Device distance vs. fraction of HC estimates (bar plot) and their detection accuracy (red dash) (CORRIDOR, CH2).

Moreover, including them would further increase space of experimental settings, whose extensive exploration presented here already entailed significant effort. Similar considerations hold for our environments; CORRIDOR and HALL have different characteristics, yet they are both indoor and in the same building. Hopefully, the results presented here will inspire similar studies in different environments and slightly different settings, improving the overall understanding of HNLOS.

On the other hand, the results we derived in §VI–§VII already cover a rich set of scenarios, inspired by practical applications, and clearly elicit several findings currently missing in the literature. Next, we distill them along with guidelines for the designers of UWB-based systems, and highlight opportunities for their exploitation in practice.

A. Distilling Findings and Guidelines

We summarize in Table VI the salient findings we extract from the many observations in §VI–§VII, structured along the main dimensions of our study, i.e., ranging reliability, ranging accuracy, and ability to detect link line-of-sight conditions. Across these dimensions, our results often show a difference in CH5 w.r.t. the other channels considered; therefore, we distinguish between general findings and channel-specific ones.

A noteworthy, cross-cutting finding across these dimensions is offered by the environments we experimented in. A narrow area (CORRIDOR) characterized by strong reflections is beneficial to ranging reliability and range, but detrimental to ranging accuracy and detection quality; a more open environment (HALL) yields directly complementary tradeoffs.

Overall, these findings highlight the primary factors affecting performance, informing the choices of the designers of UWB systems involving HNLOS. Moved by the intent to offer them concise, actionable information, we further distill guidelines for the DW1000 configuration and use (Table VII).

When these cannot be applied, alternatives are available, based on our findings. If CH5 is mandatory (e.g., due to spectrum regulations), cNLOS may be a valid alternative to cLOS$_{1024}$, depending on application requirements. Indeed, cLOS$_{1024}$ is best when ranging over short distances; cNLOS is the only option for accurate ranging at long ones, but is plagued by a large fraction of spurious estimates requiring proper filtering. Moreover, care should be taken with indicators, as CL and especially PD are high-confidence and accurate only in open (HALL) *and* CEILING deployments; otherwise, these indicators should not be relied upon in CH5.

As for optimizations, if the long preamble used in cLOS$_{1024}$ (and cNLOS) is of concern due to latency and/or energy consumption, cLOS or cMIXED can be used in CH2 or CH4. However, these are less accurate in narrow, reflective environments and at long distances, while offering comparable quality of link detection.

B. Exploiting the Findings

We argue that the findings and guidelines we distilled can find immediate use in UWB systems and applications.

For instance, the ability to reliably detect HNLOS conditions can be exploited to improve the accuracy of TDoA-based systems [4, 22]. The work in [5], tracking museum visitors with TALLA [4], reports that manually selecting the set of anchors used by avoiding those affected by human occlusions reduces the mean positioning error by 25%. Using the DW1000 indicators according to our guidelines may unlock similar improvements, yet in a fully automated way.

The ability of the DW1000 to change the radio optimization during operation, once combined with detection, unlocks the possibility of *run-time adaptation to link line-of-sight conditions*. For instance, a TWR-based system could deliver a distance estimate to the application only when the optimization used to acquire it (e.g., cLOS) matches the line-of-sight condition derived from radio indicators (e.g., LOS). Otherwise, one or more ranging exchanges can be performed to realign the two, e.g., to cater for HNLOS, improving distance estimates.

Finally, an intriguing possibility is to *combine radio optimizations and indicators with mainstream machine learning approaches*. As mentioned (§II), the latter often analyze directly the CIR, therefore completely disregarding these aspects of the radio operation. An alternative approach could include the radio optimization used and the indicator values acquired among the features considered by machine learning, increasing its accuracy and/or reducing its computational demands.

IX. CONCLUSIONS

We studied the impact on UWB ranging of the peculiar NLOS condition induced by a human body in contact with one of the link devices. This situation, hitherto largely neglected by the literature, has practical relevance in the many applications

TABLE VI
SUMMARY OF FINDINGS.

In general	CH2 and CH4	CH5
	Ranging reliability	
Ranging is more reliable, in terms of TWR exchanges successfully completed, in narrow, highly-reflective environments. Nevertheless, across all channels cNLOS reduces the fraction of useful estimates and requires proper filtering.	Low-frequency channels yield higher reliability in HNLOS at distances $\geq$20 m. CH4 is the only channel providing reliable ranging at 30 m in the open environment with weak signal reflections.	CH5 cannot be used at long distances in HNLOS, due to the attenuation combined with the higher path loss, except in a narrow environment where reflections facilitate preamble detection.
	Ranging accuracy	
HLOS yields accuracy similar to pure LOS, except when using cNLOS, due to its large underestimates. Accuracy significantly degrades in HNLOS, especially at long distances, with errors of several meters. Overall, ranging accuracy is higher in open environments less affected by signal reflections.	Sub-meter accuracy can be achieved in HNLOS with the right configuration. cLOS and cMIXED achieve it only at short distances and, when strong reflections are present, only with a CEILING deployment. cNLOS is affected by too many spurious estimates to be of practical use. Our variant cLOS$_{1024}$ is accurate at both short and long distances, in all settings.	In HNLOS, ranging is generally affected by high overestimates, especially at long distances. cLOS$_{1024}$ provides sub-meter accuracy but errors are slightly higher w.r.t. cNLOS at long distances; the latter performs worse at short distances. cLOS and cMIXED never achieve meter-level accuracy.
	Link condition detection	
Overall, CL and PD perform similarly, enabling high-confidence, correct detection. When they differ (e.g., in CH5 or when using cNLOS), CL has more HC estimates with worse accuracy, and PD the opposite. In cNLOS, the performance of CL is significantly improved by our variant, CL^*.	Indicators generally provide HC estimations, accurate across all link conditions. In some settings (e.g., LOS links in CEILING) CH2 yields fewer HC estimates, yet correct. cLOS$_{1024}$ is the optimization retaining the most stable and accurate TPR across settings; instead, cNLOS is the most unstable.	Detection is significantly less accurate in CH5, where indicators often confuse LOS and HLOS as HNLOS, especially with strong signal reflections; this is exacerbated by cNLOS. In an open environment, LOS detection approaches the one of other channels, HLOS improves but remains slightly lower.

TABLE VII
GUIDELINES FOR THE CONFIGURATION AND USE OF THE UWB RADIO.

RF channel	CH2 or CH4 are preferable, if allowed by spectrum regulations and application requirements.
Optimization	cLOS$_{1024}$, our proposed variant, yields both reliable, accurate ranging and high-confidence, accurate link condition detection, across all settings.
Indicator	CL and PD are both generally high-confidence and accurate. However, if cNLOS is used, CL must be replaced by our variant CL^*.

where users wear an UWB tag. In contrast with state-of-the-art approaches tackling generic NLOS via machine learning, we investigated whether the features available on the UWB transceiver can be *directly* exploited to *mitigate* and *detect* human occlusions. The answer is positive. An extensive experimental campaign exploring several radio, system, and deployment dimensions in two different environments is the quantitative foundation of our findings. Based on these, we distill concise guidelines for the designers of UWB-based system, enabling opportunities to unleash the full potential of this technology for human-centric applications.

ACKNOWLEDGEMENTS

This work is partially supported by the Italian government via the NG-UWB project (MIUR PRIN 2017).

REFERENCES

[1] T. Istomin *et al.*, “Janus: Dual-Radio Accurate and Energy-Efficient Proximity Detection,” *ACM IMWUT*, vol. 5, no. 4, 2022.
[2] E. Leoni *et al.*, “Measuring close proximity interactions in summer camps during the COVID-19 pandemic,” *EPJ Data Science*, 2022.
[3] “IEEE 802.15.4-2015, Standard for Low-Rate Wireless Networks.”
[4] D. Vecchia *et al.*, “TALLA: Large-scale TDoA Localization with Ultra-wideband Radios,” in *Proc. of IPIN*, 2019.
[5] F. Hachem *et al.*, “Fine-grained Stop-Move Detection in UWB-based Trajectories,” in *Proc. of PerCom*, 2022.
[6] A. Biri *et al.*, “Socitrack: Infrastructure-free interaction tracking through mobile sensor networks,” in *Proc. of MobiCom*, 2020.
[7] DecaWave Ltd., “DW1000 User Manual, version 2.18,” 2017.
[8] “DW1000 Metrics for Estimation of Non Line Of Sight Operating Conditions,” 2016.
[9] K. Wen *et al.*, “NLOS Identification and Compensation for UWB Ranging based on Obstruction Classification,” in *Proc. EUSIPCO*, 2017.
[10] Z. Zeng *et al.*, “NLOS Identification for UWB Based on Channel Impulse Response,” in *Proc. of ICSPCS*, 2018.
[11] M. Stocker *et al.*, “Performance of Support Vector Regression in Correcting UWB Ranging Measurements under LOS/NLOS Conditions,” in *Proc. of IoTBench Workshop*, 2021.
[12] Y. Cao *et al.*, “6Fit-A-Part: A Protocol for Physical Distancing on a Custom Wearable Device,” in *Proc. of ICNP*, 2020.
[13] C. Jiang *et al.*, “UWB NLOS/LOS Classification using Deep Learning Method,” *IEEE Communications Letters*, vol. 24, no. 10, 2020.
[14] S. Angarano *et al.*, “Robust Ultra-wideband Range Error Mitigation with Deep Learning at the Edge,” *Engineering Applications of Artificial Intelligence*, vol. 102, 2021.
[15] V. Barral *et al.*, “NLOS Identification and Mitigation using Low-cost UWB Devices,” *Sensors*, vol. 19, no. 16, 2019.
[16] T. Otim *et al.*, “Effects of the Body Wearable Sensor Position on the UWB Localization Accuracy,” *Electronics*, vol. 8, no. 11, 2019.
[17] A. Albaidhani *et al.*, “Ranging in UWB Using Commercial Radio Modules: Experimental Validation and NLOS Mitigation,” in *Proc. of IPIN*, 2016.
[18] “IEEE 802.15.4-2020, Standard for Low-Rate Wireless Networks.”
[19] I. Dotlic *et al.*, “Ranging Methods Utilizing Carrier Frequency Offset Estimation,” in *Proc. of WPNC*, 2018.
[20] D. Neirynck *et al.*, “Characterisation of the NLOS Performance of an IEEE 802.15.4a Receiver,” in *Proc. of WPNC*, 2015.
[21] DecaWave Ltd., “APS006 Application Note: Non Line of Sight Operation and Optimizations to Improve Performance in DW1000 Based Systems,” 2014.
[22] J. Tiemann *et al.*, “ATLAS–An Open-Source TDOA-based Ultra-Wideband Localization System,” in *Proc. of IPIN*, 2016.